peratures. The only report in the literature regarding the unfolding of insulin is by Ettinger and Timasheff,[24] although it is likely that the process was not fully reversible due to chemical decomposition. The melting transition in water is broad, having a T_m near 63 °C. In 1-octanol, the SDS–insulin complex appears to still possess its native structure, even after prolonged heating at 70 °C (>60 min). Thermal denaturation of insulin in 1-octanol displays a high degree of cooperativity. The T_m of the 6:1 SDS–insulin complex in 1-octanol has been measured, by following molar ellipticity at 222 nm, and it occurs at ∼115 °C (Figure 6), almost 50 °C above that observed in water! In addition, the T_m appears to be a function of SDS concentration, with optimal stabilization occurring in the same range as maximal apparent partitioning into 1-octanol. Therefore, it appears that proteins dissolved in nonpolar solvents may demonstrate exceptional thermal stability.

Similar increases in T_m have been observed for ribonuclease suspended in nonane versus samples in aqueous solution.[38] The T_m of ribonuclease is increased by approximately 35 °C. The lack of water in the lyophilized protein may account for its increased stability. Presumably, HIP complexes contain a similar amount of water to that of a lyophilized protein.

Unfortunately, the thermal denaturation of insulin is not reversible, preventing a thermodynamic determination of the increase in stability.[40] When heated past the T_m, the insulin rapidly

precipitates from solution. One possible explanation would be that the limited amount of water available cannot adequately solubilize the expanded volume of the unfolded state, which displays essentially no solubility in 1-octanol.

IV. Summary

Hydrophobic ion pairing represents a powerful technique for obtaining solutions of peptides and proteins in nonaqueous solvents. Complex formation involves stoichiometric addition of an anionic detergent to an aqueous solution of a protein or peptide, specific binding of the detergent to the charged residues, and precipitation from solution. This material can be redissolved in a number of organic solvents, including such nonpolar media as 1-octanol. In 1-octanol, the native structure of the protein appears to be maintained, and the material can be partitioned back into an aqueous phase, again with no loss of structure. The thermal denaturation of insulin in 1-octanol is significantly retarded, and due to the lack of water, increased chemical stability would also be predicted.[6] The applicability of hydrophobic ion pairing to other systems, especially enzymes, is being investigated. These complexes may offer distinct advantages in the delivery of therapeutically important peptides.

(40) Pace, C. N. *Trends Biotechnol.* **1990**, *8*, 93–98.

S-Aryl-L-cysteine S,S-Dioxides: Design, Synthesis, and Evaluation of a New Class of Inhibitors of Kynureninase

Rajesh K. Dua,[†] Ethan W. Taylor,[†] and Robert S. Phillips*,[‡]

Contribution from the Departments of Chemistry and Biochemistry and Department of Medicinal Chemistry and Pharmacognosy, School of Pharmacy, The University of Georgia, Athens, Georgia 30602. Received July 27, 1992

Abstract: The design, preparation, and evaluation of S-aryl-L-cysteine S,S-dioxides, a new class of potent competitive inhibitors of kynureninase from *Pseudomonas fluorescens*, are described. The most potent of these compounds, S-(2-aminophenyl)-L-cysteine S,S-dioxide, has a K_i value of 70 nM. These analogues form prominent visible absorption peaks at 500 nm, assigned to quinonoid intermediates, when bound to kynureninase. Titration of kynureninase with S-(2-aminophenyl)-L-cysteine S,S-dioxide demonstrates that 1 mol of the inhibitor is bound to the pyridoxal 5′-phosphate in each subunit. Comparative molecular field analysis of the effects of structural variation on inhibitory potency allows us to predict that the (S)-*gem*-diolate anion of L-kynurenine, a proposed reaction intermediate, binds with a K_D of 19 nM. These results provide strong additional support for the intermediacy of a *gem*-diol or *gem*-diolate anion in the reaction mechanism of kynureninase.

Introduction

Kynureninase (L-kynurenine hydrolase, EC 3.7.1.3) is a pyridoxal 5′-phosphate (PLP) dependent enzyme which catalyzes the conversion of L-kynurenine to L-alanine and anthranilic acid.[1] Kynureninase plays an important role in the catabolism of L-tryptophan in *Pseudomonas* and some other bacteria. In animals and plants, a similar enzyme, 3-hydroxykynureninase, is involved in the metabolism of L-tryptophan to L-alanine and 3-hydroxyanthranilic acid, which is further metabolized to quinolinic acid, and finally to NAD.[1] Recent research has suggested that quinolinic acid is neurotoxic and may be involved in the etiology of neurodegenerative diseases such as Huntington's chorea, epilepsy, and AIDS-related dementia.[2-4] Thus, potent and selective inhibitors of this enzyme could be of value in the treatment of these diseases. There are only a few reported inhibitors for this enzyme,

including β-chloroalanine and S-(o-nitrophenyl)-L-cysteine,[5] which are "suicide substrates". However, these compounds are relatively toxic, and they inactivate a large number of PLP-dependent enzymes. In our previous publication,[6] we have reported that (4S)- and (4R)-dihydro-L-kynurenine are potent competitive inhibitors of kynureninase, with K_i values of 0.3 μM and 1.4 μM, respectively.

[†] Department of Medicinal Chemistry and Pharmacognosy.
[‡] Departments of Chemistry and Biochemistry.

(1) Soda, K.; Tanizawa, K. *Adv. Enzymol. Relat. Areas Mol. Biol.* **1979**, *49*, 1.
(2) (a) Schwarz, R.; Okuno, E.; White, R. J.; Bird, E. D.; Whetsell, W. O. *Proc. Natl. Acad. Sci., U.S.A.* **1988**, *85*, 4079. (b) Beal, M. F.; Kowall, N. W.; Ellison, D. W.; Mazurck, M. F.; Swartz, K. J.; Martin, J. B. *Nature* **1986**, *321*, 168.
(3) Mazzari, S.; Aldinio, C.; Beccaro, M.; Toffano, G. J.; Schwarz, R. *Brain Res.* **1986**, *380*, 309.
(4) Heyes, M. P.; Brew, B. J.; Martin, A.; Price, R. W.; Salazar, A. M.; Sidtis, J. J.; Yergey, J. A.; Mouradian, M. M.; Sadler, A. E.; Keilp, J.; Rubinow, D.; Markey, S. P. *Ann. Neurol.* **1991**, *29*, 202.
(5) Kishore, G. M. *J. Biol. Chem.* **1984**, *259*, 10669.
(6) Phillips, R. S.; Dua, R. K. *J. Am. Chem. Soc.* **1991**, *113*, 7385.

S-Aryl-L-cysteine S,S-Dioxides

J. Am. Chem. Soc., Vol. 115, No. 4, 1993 1265

Table I. Competitive Inhibition of Kynureninase

compound	K_i actual (μM)	K_i predicted (μM)
S-phenyl-L-cysteine	700	113
S-phenyl-L-cysteine *S,S*-dioxide	3.9	1.13
S-(2-nitrophenyl)-L-cysteine	100	71.76
S-(2-nitrophenyl)-L-cysteine *S,S*-dioxide	23	11.19
S-(2-aminophenyl)-L-cysteine	2.5	6.04
S-(2-aminophenyl)-L-cysteine *S,S*-dioxide	0.07	0.056
S-(4-nitrophenyl)-L-cysteine *S,S*-dioxide	12	20.3
S-(4-aminophenyl)-L-cysteine	140	345
S-(4-aminophenyl)-L-cysteine *S,S*-dioxide	8.5	9.3
(2*S*,4*R*)-dihydrokynurenine	1.4[a]	0.88
(2*S*,4*S*)-dihydrokynurenine	0.3[a]	0.33
(2*S*,4*R*)-*gem*-diolate reaction intermediate		0.03
(2*S*,4*S*)-*gem*-diolate reaction intermediate		0.019

[a] From ref 6.

We proposed that this strong inhibition was due to the structural similarity of these compounds with the *gem*-diolate anion formed from kynurenine, which is a postulated reaction intermediate.[7] We reasoned that other structural analogues of this intermediate would also be potent inhibitors of kynureninase. Now, we report that *S*-aryl-L-cysteine *S,S*-dioxides are a new class of potent inhibitors of kynureninase. To develop a 3D-QSAR for the enzyme inhibition, the method of comparative molecular field analysis (CoMFA) was used. This approach permits the inclusion of structurally dissimilar compounds within a single QSAR study.[8] CoMFA correlates biological activities of compounds with their three-dimensional structural properties, as represented by their steric and electrostatic fields sampled at points in a lattice or grid spanning a three-dimensional region. This analysis has also allowed us to estimate the binding affinity for the proposed reaction intermediate. These results provide further strong support for the intermediacy of a *gem*-diol or *gem*-diolate anion of kynurenine in the kynureninase reaction mechanism.

Results

Chemistry. *S*-Phenyl-L-cysteine was synthesized enzymatically following the procedure of Esaki et al.,[9] by incubating thiophenol with L-serine in the presence of the $\alpha_2\beta_2$ complex of *Salmonella typhimurium* tryptophan synthase. The *S*-(nitrophenyl)-L-cysteines were readily prepared by the S_NAr reaction of 2-fluoro- and 4-fluoronitrobenzene with L-cysteine in dimethylformamide containing triethylamine.[10] Reduction of both isomers of *S*-(nitrophenyl)-L-cysteine was accomplished by stirring with Zn in acetic acid. The oxidation of the cysteinyl thioethers to *S,S*-dioxides was achieved by using a procedure described by Goodman et al.[11] with slight modifications. This method produced good results when the aryl cysteines were treated with a mixture of 98% formic acid and 30% hydrogen peroxide. However, when 88% formic acid was used for this reaction, a slightly impure product was obtained, and the yields were also lower. Earlier work on these compounds indicated that it was not possible to oxidize *S*-(aminophenyl)-L-cysteines to *S,S*-dioxides without degradation; indeed, it was suggested that these sulfones were inherently unstable.[11] We found that the rate of sulfone formation strongly depends on the position of the nitro group on the ring. When the nitro group is present at the ortho position, the reaction took 48 h or more to reach completion; however, when the ring is unsubstituted or the nitro group is present at the para-position, the reaction was over within 12 h. Reduction of the nitrophenyl sulfones was uneventfully performed by catalytic hydrogenation
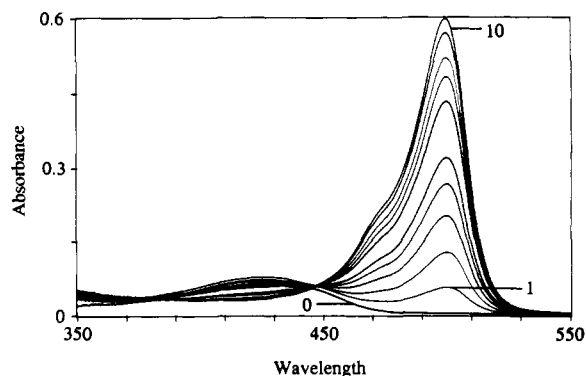
(7) Braunstein, A. E.; Shemyakin, M. M. *Biokhimiya (Moscow)* **1953**, *18*, 393.

(8) Cramer, R. D., III; Patterson, J. D.; Bunce, J. D. *J. Am. Chem. Soc.* **1988**, *110*, 5959.

(9) Esaki, N.; Tanaka, H.; Miles, E. W.; Soda, K. *Agric. Biol. Chem.* **1983**, *47* (12), 2861.

(10) Phillips, R. S.; Ravichandran, K.; Von Tersch, R. L. *Enzyme Microb. Technol.* **1989**, *11*, 80–83.

(11) Goodman, L.; Ross, L. O.; Baker, B. R. *J. Org. Chem.* **1958**, *23*, 1251.

Figure 1. Rapid-scanning spectra of kynureninase in the presence of *S*-(2-aminophenyl)-L-cysteine *S,S*-dioxide. Spectra were collected at (1) 0.0105 s; (2) 0.021 s; (3) 0.0315 s; (4) 0.042 s; (5) 0.0525 s; (6) 0.084 s; (7) 0.105 s; (8) 0.126 s; (9) 0.168 s; and (10) 0.210 s. Curve 0 is the spectrum of the enzyme alone.
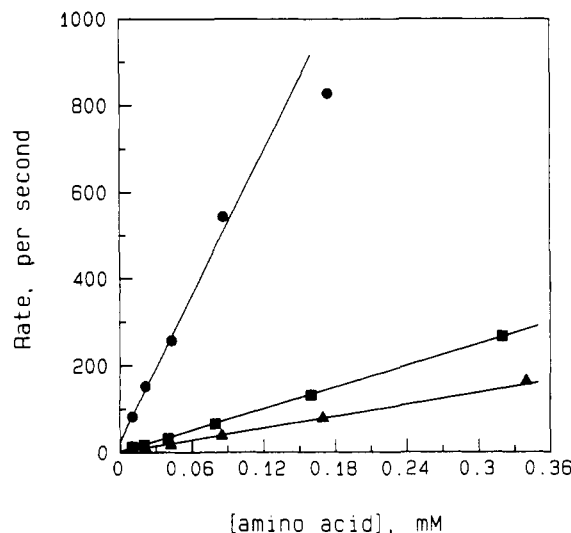

Figure 2. Plot of apparent rate constant for formation of the 500-nm intermediate against concentration of inhibitor: (●) *S*-(2-aminophenyl)-L-cysteine; (■) *S*-(2-aminophenyl)-L-cysteine *S,S*-dioxide; (▲) *S*-phenyl-L-cysteine *S,S*-dioxide.

with 10% Pd/C using formic acid as solvent to give the desired *S*-(aminophenyl)-L-cysteine *S,S*-dioxides.

Inhibition. The results of competitive inhibition studies by *S*-aryl-L-cysteines and *S*-aryl-L-cysteine *S,S*-dioxides are shown in Table I. *S*-Phenyl-L-cysteine was found to be a weak inhibitor, with a K_i value of 700 μM; however, its oxidized analogue, *S*-phenyl-L-cysteine *S,S*-dioxide, showed a 180-fold decrease in its K_i value to 3.9 μM. Similarly, substitution by an ortho amino group, in *S*-(2-aminophenyl)-L-cysteine, showed a 318-fold decrease in its K_i value to 2.5 μM. The compound which combines both of these structural features, *S*-(2-aminophenyl)-L-cysteine *S,S*-dioxide, turned out to be the most potent competitive inhibitor of kynureninase known, with a K_i value of 70 nM. In contrast, the presence of a para amino substituent did not result in substantial improvement in binding. A similar, but less significant, improvement in the activity of the compounds was observed by sulfone formation in the cases of the 2-nitro, 4-nitro, and 4-amino compounds (Table I).

Spectroscopic Studies. Addition of *S*-phenyl-L-cysteine, *S*-(2-aminophenyl)-L-cysteine, *S*-phenyl-L-cysteine *S,S*-dioxide, or *S*-(2-aminophenyl)-L-cysteine *S,S*-dioxide to solutions of kynureninase results in rapid formation of an intense absorption peak at 500 nm assigned to a quinonoid carbanionic intermediate (Figure 1), with concomitant reduction of the 420-nm peak due to the enzyme-bound pyridoxal 5'-phosphate. The rate constant for formation of the 500-nm peak increases linearly with concentration for *S*-(2-aminophenyl)-L-cysteine, *S*-phenyl-L-cysteine *S,S*-dioxide, and *S*-(2-aminophenyl)-L-cysteine *S,S*-dioxide (Figure

Table II. Rate Constants for Reaction of S-Arylcysteines with
Kynureninase

compound	k_f/K_D (M^{-1} s^{-1})	k_r (s^{-1})	$k_r/(k_f/K_D)$ (μM)
S-phenyl-L-cysteine S,S-dioxide	4.5×10^5	2	4.4
S-(2-aminophenyl)-L-cysteine	5.6×10^6	24	4.3
S-(2-aminophenyl)-L-cysteine S,S-dioxide	8.0×10^5	4.8	5.9

2), but is too rapid to measure (i.e., completed within the dead time of the stopped-flow instrument) for S-phenyl-L-cysteine. The observed linear dependence of the apparent rate constant on ligand concentration suggests that this reaction is a second-order process under pseudo-first-order conditions; however, for quinonoid complex formation with tryptophan indole-lyase and other PLP-dependent enzymes, it has been shown that an amino acid PLP-Schiff's base (E·L) is an obligatory intermediate in the formation of quinonoid complexes (E·L$_Q$)[12] (eq 1).
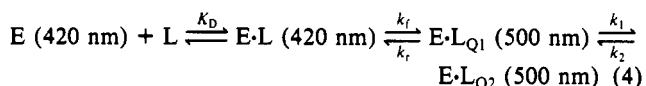
$$E \ (420 \ nm) + L \xrightleftharpoons{K_D} E{\cdot}L \ (420 \ nm) \xrightleftharpoons[k_r]{k_f} E{\cdot}L_Q \ (500 \ nm) \quad (1)$$
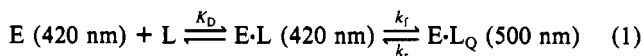
The dependence of the relaxation time on the concentration of ligand for the mechanism of eq 1 is given in eq 2.[13] However, if [L] $\ll$ K_D, eq 2 will reduce to eq 3, which predicts a linear

$$1/\tau_1 = k_f[L]/(K_D + [L]) + k_r \quad (2)$$

$$1/\tau_1 = (k_f/K_D)[L] + k_r \quad (3)$$

concentration dependence, as observed in Figure 2. The values of k_f/K_D and k_r obtained from the slopes and intercepts of Figure 2 are given in Table II. The overall equilibrium constant for ligand binding, equivalent to K_i, for the mechanism shown in eq 1 can be calculated from the ratio of k_r and k_f/K_D. This calculated K_i value is in good agreement with the kinetically derived K_i value in Table I for S-phenyl-L-cysteine S,S-dioxide and S-(2-aminophenyl)-L-cysteine, but is about 85-fold higher for S-(2-aminophenyl)-L-cysteine S,S-dioxide. This suggests that another complex may be forming for the latter compound; indeed, the absorbance increase at 500 nm for this compound is biphasic. At low ligand concentrations (10–20 μM), the second phase has a large amplitude (50–70%), but the amplitude of the second phase diminishes to less than 2% at 180 μM. Although slow second phases are also observed in the reactions of the other S-arylcysteines, they are observed only at the highest concentrations and are always of low amplitude, suggesting that they do not significantly contribute to the overall binding. Thus, for the binding of S-(2-aminophenyl)-L-cysteine S,S-dioxide, the mechanism must be extended to include an additional quinonoid intermediate, as shown in eq 4. This mechanism predicts that the

$$E \ (420 \ nm) + L \xrightleftharpoons{K_D} E{\cdot}L \ (420 \ nm) \xrightleftharpoons[k_r]{k_f} E{\cdot}L_{Q1} \ (500 \ nm) \xrightleftharpoons[k_2]{k_1}$$
$$E{\cdot}L_{Q2} \ (500 \ nm) \quad (4)$$

rate of the slow second phase will be independent of the ligand concentration (eq 5), as we have observed. The average value

$$1/\tau_2 = k_1 + k_2 \quad (5)$$

of the rate constant for the second relaxation is 11 s^{-1}. Since the K_i determined in the steady-state experiments is 85-fold lower than that calculated from the two-step mechanism, $K_1 = k_1/k_2 \simeq 85$. The observed relaxation is the sum of k_1 and k_2 (eq 5); thus, k_1 = 10.87 s^{-1} and k_2 = 0.13 s^{-1}.

The strong binding of S-(2-aminophenyl)-L-cysteine S,S-dioxide makes it an ideal titrant for kynureninase. Addition of even substoichiometric amounts of S-(2-aminophenyl)-L-cysteine S,-S-dioxide to kynureninase results in a strong absorbance at 500 nm (Figure 3). However, at low concentrations of S-(2-aminophenyl)-L-cysteine S,S-dioxide, the absorbance peak is not
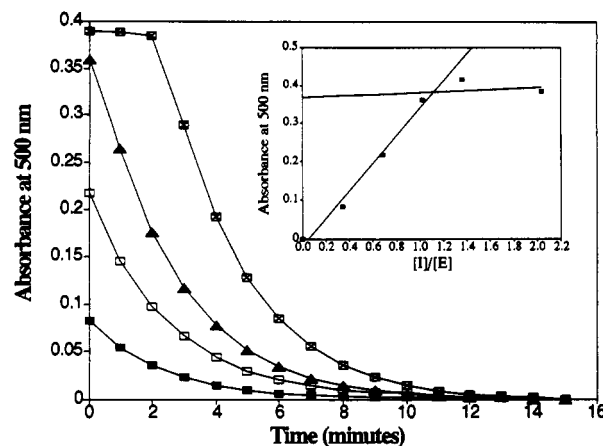
Figure 3. Plot of absorbance at 500 nm vs time for the complex of S-(2-aminophenyl)-L-cysteine S,S-dioxide and kynureninase (9.8 μM): (■) 3.33 μM S-(2-aminophenyl)-L-cysteine; (□) 6.67 μM; (▲) 10.0 μM; (squares with X) 20.0 μM. Inset: Initial absorbance at 500 nm plotted against the ratio of inhibitor and enzyme concentration.
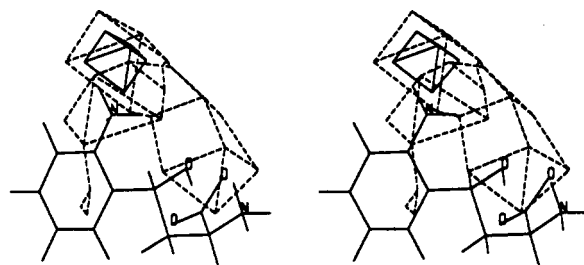
Figure 4. CoMFA steric field graph around (4S)-dihydro-L-kynurenine.
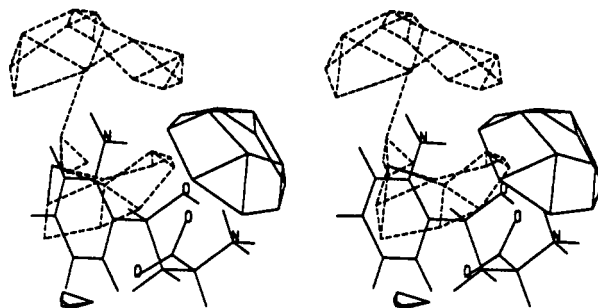
Figure 5. CoMFA electrostatic field graph around (4S)-dihydro-L-kynurenine.

stable but decays slowly in a first-order process, with a rate constant of 0.4 min^{-1} at 25 °C which is independent of ligand concentration (Figure 3). The quinonoid complexes formed from the other arylcysteines and S,S-dioxides are also unstable and decay much more rapidly. This decay likely reflects the irreversible β-elimination of the aryl thiolate or sulfinate ion from the quinonoid intermediate. The elimination of 2-nitrothiophenolate ion from S-(2-nitrophenyl)-L-cysteine catalyzed by *Pseudomonas marginalis* kynureninase has been previously demonstrated.[3] Furthermore, we obtained evidence for pyruvate ion formation by β-elimination in the reaction of S-(2-nitrophenyl)-L-cysteine S,S-dioxide by coupling with lactate dehydrogenase and NADH (data not shown). A plot of the initial absorbance at 500 nm against the stoichiometric ratio of [I]/[E] (inset in Figure 3) gives a sharp break at about 1.05 mol of ligand bound per subunit of 50 kDa; thus, one molecule of the inhibitor is bound to each active site of kynureninase. The observed molar extinction coefficient, ϵ = 3.9 $\times$ 10^4 M^{-1} cm^{-1}, is consistent with the intensity of quinonoid complexes observed with *Escherichia coli* tryptophan indole-lyase[12] and in model systems.[14] These data suggest that one

(12) Phillips, R. S. *Biochemistry* **1991**, *30*, 5927.
(13) Strickland, S.; Palmer, G.; Massey, V. *J. Biol. Chem.* **1975**, *250*, 4048.

(14) Metzler, C. M.; Harris, A. G.; Metzler, D. E. *Biochemistry* **1988**, *27*, 4923.

Scheme I

anthranilic acid + L-alanine

Kynureninase

I II

H₂O

III

IA IIA

(slow)

IIIA
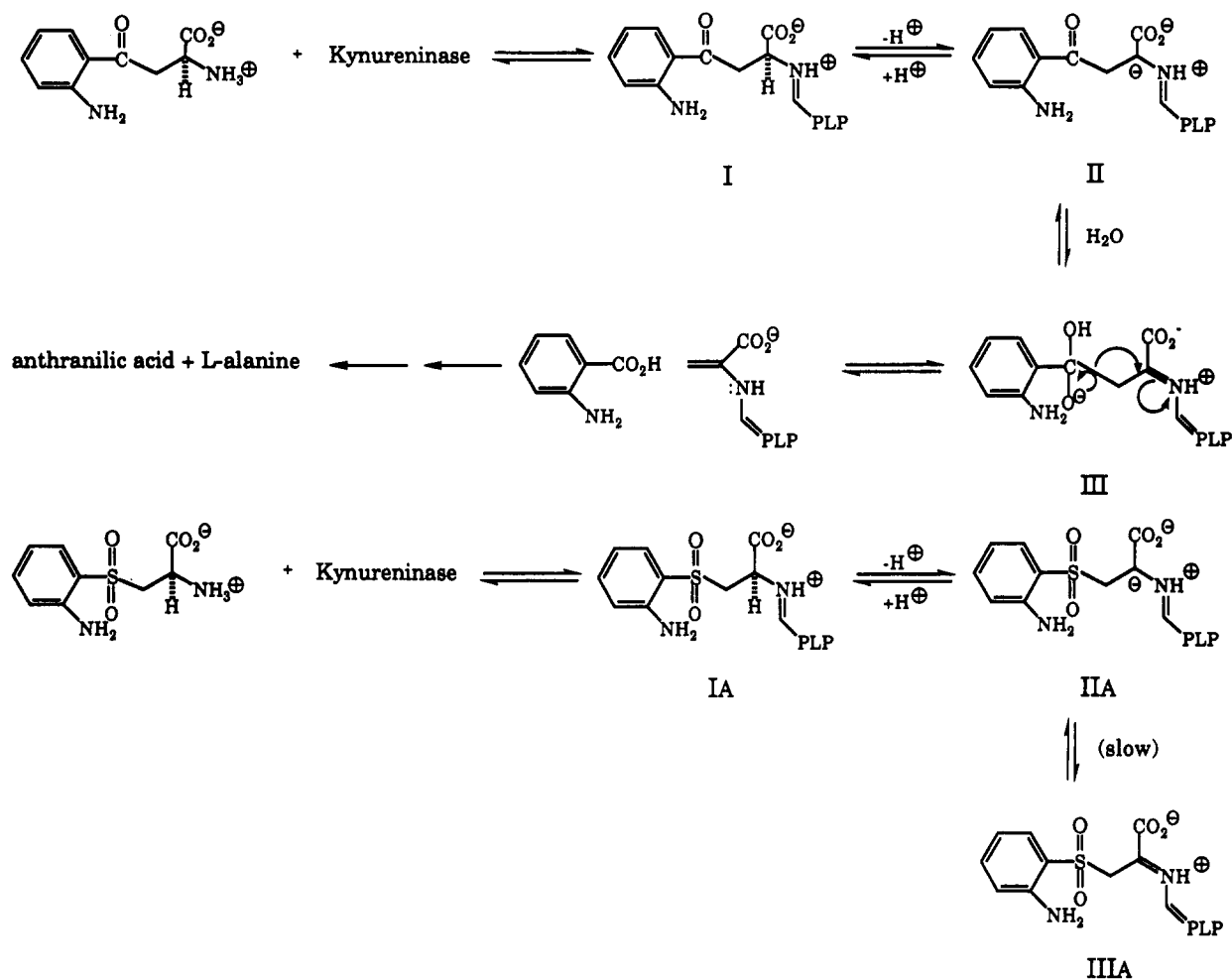
PLP is bound to each subunit and are in contrast to the report of Moriguchi et al.[15] that kynureninase from *P. marginalis* contains only 1 mol of PLP per mol of dimeric enzyme.

Comparative Molecular Field Analysis. Figure 4 shows the alignment of a representative group of the inhibitor molecules.[16] The global minimum-energy conformation of the potent (4*S*)-isomer of dihydro-L-kynurenine was used as the template for the alignment of the set of inhibitor molecules. This choice was unambiguous, as the conformational search clearly demonstrated a strong preference for this particular conformation (i.e., there were no other significantly different minima within several kcal/mol of this one). The other analogues were aligned using an essentially identical conformation in a number of cases. Attempts to perform CoMFA using a least squares fit of the global minimum for each molecule did not produce a correlation, apparently due to too much inconsistency in the conformational variables for the phenyl ring and the amino acid portion.

An initial PLS analysis was run in order to determine that the optimum number of components was two and the crossvalidated

r^2, which was 0.5. As has been noted elsewhere,[17,18] a crossvalidated r^2 of 0.3 corresponds to a probability of chance correlation with activity of <0.05; thus the current results are definitely significant. This number of components gave a final model with conventional $r^2 = 0.903$, $s = 0.413$, $n = 11$, $F_{2,8} = 37.03$, and $p < 0.001$. Actual vs predicted pK_i values from this 3D-QSAR model are listed in Table I. The results of a CoMFA are best interpreted as CoMFA electrostatic and steric field graphs. These graphs show regions in space around the molecules as contoured "chicken wire" volumes, where specific steric or electrostatic interactions enhance or detract from the activity.

Figure 4 is a three-dimensional plot of the steric field graph around 4*S*-dihydro-L-kynurenine. In this graph, occupation of the region encompassed by broken lines reduces the activity of an inhibitor, whereas steric bulk protruding into the regions contoured with solid lines increases the activity of an inhibitor. This graph shows that there is an optimal size for the ortho substituent; apparently, the amino group is near optimal, as just outside the solid-line-contoured region is a negative steric region, suggesting that increasing the size from an amino to a nitro group produces a significant reduction in activity.

Figure 5 shows the CoMFA electrostatic field graph, again with the 4*S*-dihydro-L-kynurenine structure shown for reference. In this graph, the presence of positive potential in the region contoured with broken lines or the presence of negative potential in the region contoured with solid lines contributes to the activity of inhibitors in the 3D-QSAR model. The opposite type of potential in either of these regions should reduce activity. As can be seen in Figure

(15) Moriguchi, M.; Yamamoto, T.; Soda, K. *Biochemistry* **1973**, *12*, 2969.

(16) CoMFA descriptors are the magnitude of either the steric or the electrostatic potential exerted by the atoms in the set of molecules on a proton probe, sampled at the points in the region surrounding the aligned molecules. The resulting data set is analyzed by the partial least squares (PLS) method, which, unlike multiple linear regression, permits the analysis of tables with many more columns than rows. Statistical crossvalidation is used to check the validity of model equations which correlate the biological or dependent property with the physical parameters of the drug molecules. Crossvalidation tests a model by omitting compounds (rows), rederiving the model, and then predicting the activity of the omitted compounds, thus simulating the prediction of the "real world" outside the training set. As a result of these statistical analyses, a model is developed for the properties of drug molecules and is optimized for predicting the biological activity of new analogues.

(17) Clark, M.; Cramer, R. D., III; Jones, D. M.; Patterson, D. E.; Simeroth, P. E. *Tetrahedron Comput. Methodol.* **1990**, *3*, 47.

(18) Thomas, B. F.; Compton, D. R.; Martin, B. R.; Seamus, S. F. *Mol. Pharmacol.* **1991**, *40*, 656.

1268   *J. Am. Chem. Soc., Vol. 115, No. 4, 1993*

Dua et al.

5, a region of positive potential is situated around the ortho amino substituent. This suggests that electrostatic interactions, possibly hydrogen bonding, of this substituent contribute to the binding of these inhibitors (and kynurenine as well). Placement of an ortho nitro substituent, with a negative potential, has unfavorable electrostatic interactions. Another notable feature includes an asymmetrically placed negative potential region in the region of the alcohol oxygen of the 4S-dihydro-L-kynurenine structure, consistent with the position of the anionic oxygen in the hypothetical *gem*-diolate reaction intermediate having the (S) absolute stereochemistry as proposed previously.[6] CoMFA allows us to estimate the binding affinity for the enantiomeric *gem*-diolate anions formed by addition of hydroxide ion to L-kynurenine (Table I).

Discussion

The mechanism of action of kynureninase has been of considerable interest for more than 40 years, due to the unusual nature of the β-substitution reaction, which is *electrophilic* rather than nucleophilic in character. Although some of the early mechanisms were postulated to involve implausible redox chemistry[19] or transamination,[20] Braunstein proposed the involvement of hydroxide ion attacking the carbonyl.[7] More recently, a mechanism was proposed involving attack at the carbonyl by an enzyme nucleophile, resulting in a transient acylenzyme intermediate.[21] Tanizawa and Soda studied the retro-aldol cleavage of dihydrokynurenine catalyzed by kynureninase and concluded that their results supported a mechanism similar to that of Braunstein, with a *gem*-diol intermediate.[22]   Recently, we studied the stereochemistry of reaction and competitive inhibition of *Pseudomonas fluorescens* kynureninase with the separated diastereomers of dihydro-L-kynurenine, and we also concluded that the reaction must proceed via a *gem*-diolate anion intermediate.[6] On the basis of these results, we wished to obtain further support for a *gem*-diolate intermediate of L-kynurenine in the reaction of kynureninase. Given the mechanistic considerations presented above, we reasoned that analogues containing the sulfone group, SO₂, in place of the carbonyl should be potent inhibitors of kynureninase. A series of S-aryl-L-cysteines and their corresponding S,S-dioxides were prepared and their interactions with kynureninase evaluated.

All of these compounds are competitive inhibitors of kynureninase (Table I). However, the presence of the sulfone group or an ortho amino group dramatically increases the binding affinity (Table I). Furthermore, these effects are additive, and S-(2-aminophenyl)-L-cysteine S,S-dioxide has a K_i value of 70 nM, some 350-fold lower than the K_m for kynurenine. This compound is by far the most potent competitive inhibitor for kynureninase discovered to date.

To achieve a greater understanding of the mechanism of interaction of these compounds with kynureninase, rapid-scanning and single-wavelength stopped-flow kinetic studies were performed with S-phenyl-L-cysteine S,S-dioxide, S-(2-aminophenyl)-L-cysteine, and S-(2-aminophenyl)-L-cysteine S,S-dioxide. All of these compounds form quinonoid carbanionic intermediates, with intense peaks at 500 nm, upon mixing with kynureninase (Figure 1); the estimated K_i values calculated from the obtained rate constants for quinonoid intermediate formation and reprotonation are in excellent agreement with the measured K_i values for S-phenyl-L-cysteine S,S-dioxide and S-(2-aminophenyl)-L-cysteine, indicating a simple two-step binding mechanism occurs. However, for S-(2-aminophenyl)-L-cysteine S,S-dioxide, the kinetic data indicate a three-step mechanism, with the third step contributing about 85-fold to the overall binding affinity. This third step appears to be a slow conformational change of the initial quinonoid intermediate that requires the presence of both the ortho amino

and the sulfone substituents to be observed. Slow conformational changes have been frequently observed in the binding of "transition state analogue" inhibitors[23] and are presumably related to the slow formation of an enzyme conformation which normally binds to the transition state (or high-energy intermediate) of the reaction.

The proposed mechanism of kynureninase is presented in Scheme I. L-Kynurenine binds to form a Schiff's base with the PLP cofactor (I), that is subsequently deprotonated at the α-carbon to yield the quinonoid intermediate (II). Preliminary rapid-scanning and single-wavelength stopped-flow studies of the reaction of kynureninase with L-kynurenine show rapid (within the dead time of the stopped-flow instrument, ca. 1 ms) formation of a transient intermediate with λ_{max} at 494 nm, as expected for a quinonoid structure (R. S. Phillips, unpublished observations). This very high rate of deprotonation suggests that subsequently the carbonyl group is hydrated, with assistance from a general base in the active site, to give the *gem*-diolate anion of the quinonoid intermediate (III). This intermediate can then undergo a retro-Claisen condensation to give the anthranilic acid and, ultimately, L-alanine products. Our 3D-QSAR analysis of the binding affinity of the series of arylcysteines, arylcysteine S,S-dioxides, and dihydro-L-kynurenines allows us to predict the K_d values for binding of the enantiomeric *gem*-diolates of kynurenine to kynureninase from solution. As we predicted previously on the basis of stereochemical arguments,[6] the (S)-*gem*-diolate has the strongest estimated affinity, with an estimated K_d value of 19 nM, while the (R)-enantiomer is predicted to have a K_d of 30 nM (Table I).

The binding of S-(2-aminophenyl)-L-cysteine S,S-dioxide to kynureninase also proceeds through initial formation of a Schiff's base intermediate (IA in Scheme I) and a quinonoid intermediate (IIA), which slowly isomerizes to a second quinonoid intermediate (IIIA). This second quinonoid intermediate would be the analogue of the *gem*-diolate quinonoid structure, III, in the kynurenine reaction mechanism. The overall binding constant for this sulfone inhibitor, 70 nM, is only 3.5-fold greater than that predicted from the 3D-QSAR for the binding of the (S)-*gem*-diolate anion of L-kynurenine. Thus, this sulfone is within 0.77 kcal at 25 °C of being a "perfect" analogue of the proposed *gem*-diolate anion reaction intermediate. The slow decomposition of the quinonoid complex of S-(2-aminophenyl)-L-cysteine S,S-dioxide (Figure 3) occurs via a β-elimination of the aryl sulfone to produce, presumably, 2-aminobenzenesulfinic acid and ammonium pyruvate. The catalysis of β-elimination reactions by kynureninase has been previously demonstrated by Kishore[5] and results in irreversible inactivation. However, in those reactions and in the reactions of the S-(nitrophenyl)-L-cysteine S,S-dioxides which we examined, the β-eliminations exhibit a very high rate (2000–6000 min⁻¹), whereas the β-elimination of S-(2-aminophenyl)-L-cysteine S,S-dioxide occurs at 0.4 min⁻¹. This 5000-fold or greater stabilization of the quinonoid intermediate toward the β-elimination reaction is probably also a reflection of the binding of S-(2-aminophenyl)-L-cysteine S,S-dioxide as an "intermediate state analogue" inhibitor of kynureninase. These results suggest that the sulfone group may be generally useful in the design of potent inhibitors of enzymes which proceed via hydrated tetrahedral intermediates.[24]

Experimental Section

Instrumentation. UV and visible spectra as well as steady-state kinetic measurements and coupled assays were performed on a Gilford Response II spectrophotometer, equipped with a Peltier-type thermoelectric cell block for temperature control. ¹H NMR spectra were obtained in D₂O containing DCl on a Bruker AC-300 spectrometer at 300.13 MHz. FT-IR spectra were obtained on a Perkin Elmer Model 1600 FT-IR. Rapid-scanning and single-wavelength stopped-flow kinetic measurements were performed as previously described.[12]

Preparation of Kynureninase. The cells of *P. fluorescens* (ATCC 11250) were grown as described by Hayaishi and Stanier[25] in a minimal

(19) Longenecker, J. B.; Snell, E. E. *J. Biol. Chem.* **1955**, *213*, 229.
(20) Dalgliesh, C. E.; Knox, W. E.; Neuberger, A. *Nature* **1951**, *168*, 20.
(21) Akhtar, M.; Emery, V. C.; Robinson, J. A. In *The Chemistry of Enzyme Action*; Page, M. I., Ed.; New Comprehensive Biochemistry, Vol. 6; Elsevier: New York, 1983; pp 303–372.
(22) Tanizawa, K.; Soda, K. *J. Biochem.* (*Tokyo*) **1979**, *86*, 1199.

(23) Morrison, J.; Walsh, C. T. *Adv. Enzymol. Relat. Areas Mol. Biol.* **1988**, *61*, 201.
(24) The results presented herein have been submitted in a patent application: Inhibitors of Kynureninase. US 07/689,705, April 18, 1991.

medium containing 0.1% L-tryptophan as the sole carbon and nitrogen source. From 100 L of medium, grown for 18 h at 30 °C, was obtained 230 g of wet cell paste. The cells were suspended in 1 L of 0.01 M potassium phosphate, pH 7.0, and disrupted by two passages through a Manton–Gaulin homogenizer. Kynureninase was purified from crude cell extracts by a modification of the procedure of Moriguchi and Soda.[26] The purified enzyme exhibited a specific activity of 10 μmol/(min mg) with L-kynurenine in 0.1 M potassium phosphate buffer at pH 7.8 and 25 °C.

Assays of Kynureninase. Kynureninase activity was measured by following the decrease in absorbance at 360 nm ($\Delta\epsilon = -4500$ M^{-1} cm^{-1}) due to formation of anthranilic acid. A typical assay mixture contained 0.4 mM L-kynurenine in 0.04 M potassium phosphate, pH 7.8, containing 40 μM pyridoxal 5'-phosphate, at 25 °C. The reactions of arylcysteines and arylcysteine S,S-dioxides with kynureninase were performed using a coupled spectrophotometric assay with lactate dehydrogenase and NADH, by monitoring the decrease in absorbance at 340 nm ($\Delta\epsilon = -6200$ M^{-1} cm^{-1}) due to pyruvate ion formation. The competitive inhibition of these compounds was determined by variation of L-kynurenine concentrations at several fixed values of the compound. K_m and V_{max} values were calculated by fitting of initial rate data to the Michaelis–Menten equation with ENZFITTER (Elsevier) on a Zenith Z-286 personal computer. K_i values were determined from eq 6.[27]

$$\nu = V_{max}[S]/(K_m(1 + [I]/K_i) + [S]) \qquad (6)$$

Molecular Modeling and Structure Alignment. The set of 11 kynureninase inhibitors as well as 2 hypothetical enzyme reaction intermediates were modeled with SYBYL 5.4 (Tripos Associates, St. Louis, MO). Low-energy conformations were determined by molecular mechanics, with systematic search of torsional space (MAXIMIN and SEARCH options of SYBYL), using the unmodified TRIPOS molecular mechanics force field.[28] Atomic charges on the zwitterionic forms (electrically neutral) were calculated using the MNDO method. Considerations leading to the chosen alignment of the inhibitor molecules are discussed in the Results section.

The CoMFA option in SYBYL/QSAR was used to develop a 3D-QSAR for the present set of 13 kynureninase inhibitors listed in Table I. Electrostatic (Coulombic) and steric (Lennard-Jones) potentials (evaluated as interactions with a probe sp^3 carbon atom) were sampled for a grid of points in space around the set of molecules. The CoMFA grid spacing was 2 Å in all three dimensions within the defined region, which extended beyond the van der Waals envelopes of all the molecules. A table was built with the compounds as rows and having two types of column values: pK_i vs kynureninase (dependent variable) and the steric and electrostatic field potential values (independent variables). PLS analysis runs produced model equations explaining the target property (pK_i) in terms of the independent variables. The optimum number of components in the final PLS model was determined by crossvalidation, which also yields a crossvalidated r^2 value. Plots of the CoMFA steric and electrostatic fields around the molecules (Figures 4 and 5) permit the visualization of the 3-D molecular properties which determine enzyme activity. The derived 3D-QSAR model was used to predict the affinity (pK_i) of the isomers of the hypothetical anionic *gem*-diolate anion enzyme reaction intermediate, which would be expected to have an affinity comparable to those of the best inhibitors designed using this structure as a model.

Synthesis. A. Preparation of S-Phenyl-L-cysteine. A mixture containing 1.23 mL (12 mmol) of thiophenol, 0.525 g (5 mmol) of L-serine, 10 mM potassium phosphate buffer, pH 7.8, 0.13 mg (20 nmol) of pyridoxal 5'-phosphate, and 5 mg of *S. typhimurium* tryptophan synthase in a total volume of 25 mL was stirred at 37.5 °C. After 48 h, the reaction mixture was cooled to 4 °C, and the thick white precipitate was filtered and washed with water and then ethanol to give 0.31 g (32%) of white crystals, mp 198–200 °C dec (lit.[11] 190 °C). UV (0.01 M HCl): $\lambda_{max} = 251$ nm (log $\epsilon = 3.77$). ¹H NMR (D₂O, DCl): δ 2.8–3.0 (2 H, m, β-CH₂), 3.62–3.67 (1 H, dd, α-CH), 6.7–6.9 (5 H, m, aromatic). $[\alpha]^{23}_D$ +66.77 ($c = 0.63$, 1 M HCl).

B. Preparation of S-(2-Nitrophenyl)-L-cysteine. To a flask containing 5 g of L-cysteine (28.5 mmol), 4.47 g of 2-fluoronitrobenzene (28.5 mmol), and 20 mL of DMF was added 7.84 mL of triethylamine. After being stirred at room temperature for 3 h, the contents of the flask solidified into a thick yellow cake. This solid was broken in 20 mL of

water and filtered to give the crude product, which was recrystallized from hot water to yield 4.75 g (69%) of yellow crystals, mp 177–178 °C (lit. 164 °C).[29] UV (0.01 M HCl): $\lambda_{max} = 243$ nm (log $\epsilon = 4.11$); 370 nm (log $\epsilon = 3.44$). ¹H NMR (D₂O, DCl): δ 3.3 (1 H, dd, β-CH₂), 3.55 (1 H, dd, β-CH₂), 4.1 (1 H, dd, α-CH), 7.1–7.9 (4 H, m, aromatic). $[\alpha]^{23}_D$ +59.3 ($c = 0.356$, 1 M HCl).

C. Preparation of S-(4-Nitrophenyl)-L-cysteine. This compound was prepared as described for S-(2-nitrophenyl)-L-cysteine, using 4-fluoronitrobenzene. The crude product was recrystallized from hot water to yield 4.5 g (65%) of yellow crystals, mp 170–172 °C (lit. 173–175 °C).[29] UV (0.01 M HCl): $\lambda_{max} = 335$ nm (log $\epsilon = 4.02$). ¹H NMR (D₂O, DCl): δ 3.4–3.6 (2 H, m, β-CH₂), 4.15 (1 H, dd, α-CH), 7.3–7.9 (4 H, dd, aromatic). $[\alpha]^{23}_D$ +48.8 ($c = 1.25$, 1 M HCl).

D. Preparation of S-(2-Aminophenyl)-L-cysteine. S-(2-nitrophenyl)-L-cysteine (0.26 g, 1.07 mmol) was dissolved in 25 mL of acetic acid, and 1.0 g of zinc powder was added. The mixture was stirred at room temperature overnight. After completion of the reaction, the solid was filtered off onto Celite, and the filtrate was concentrated in vacuo to give an oil. This oil was triturated with water and methanol to give 0.19 g (83%) of a cream-colored solid, mp 225–228 °C dec (lit. 240 °C rac).[11] ¹H NMR analysis indicated that this product was greater than 98% pure. UV (0.01 M HCl): $\lambda_{max} = 253$ nm (log $\epsilon = 3.70$); 295 (sh) (log $\epsilon = 2.92$). ¹H NMR (D₂O, DCl): δ 3.51–3.65 (2 H, m, β-CH₂), 4.26–4.29 (1 H, dd, α-CH), 7.4–7.8 (4 H, m, aromatic). $[\alpha]^{23}_D$ +60.2 ($c = 1.12$, 1 M HCl).

E. Preparation of S-(4-Aminophenyl)-L-cysteine. S-(4-Nitrophenyl)-L-cysteine (0.9 g, 3.7 mmol) was reduced in 100 mL of acetic acid with 5.0 g of zinc dust as described for S-(2-aminophenyl)-L-cysteine. Workup gave 0.7 g of an off-white solid, which contained some minor impurities, as determined by ¹H NMR analysis. Recrystallization from hot ethanol gave 0.59 g (75%) of off-white crystals. UV (0.01 M HCl): $\lambda_{max} = 253$ nm (log $\epsilon = 3.58$). ¹H NMR (D₂O, DCl): δ 3.57 (2 H, m, β-CH₂), 4.2 (1 H, dd, α-CH), 7.3–7.6 (4 H, m, aromatic). $[\alpha]^{23}_D$ = +0.19 ($c = 1.03$, 1 M HCl).

F. Preparation of S-Phenyl-L-cysteine S,S-Dioxide. S-Phenyl-L-cysteine (0.2 g, 1 mmol) was dissolved in a mixture of 5 mL of 98% formic acid and 2 mL of 30% hydrogen peroxide and stirred at room temperature for 12 h. After completion of the reaction, the solvent was carefully evaporated in vacuo at 25–30 °C and the residue recrystallized from water to give 0.18 g (77%) of a white solid, mp 153–156 °C (lit. 155–156 °C).[11] UV (0.01 M HCl): $\lambda_{max} = 266$ nm (log $\epsilon = 3.02$); 273 nm (log $\epsilon = 2.95$). IR (Nujol mull): ν 1154 and 1303 cm^{-1} (SO₂). ¹H NMR (D₂O, DCl): δ 3.9–3.98 (2 H, m, β-CH₂), 4.46–4.49 (1 H, dd, α-CH), 7.54–7.87 (5 H, m, aromatic). $[\alpha]^{23}_D$ +21.2 ($c = 0.52$, 1 M HCl).

G. Preparation of S-(2-Nitrophenyl)-L-cysteine S,S-Dioxide. S-(2-Nitrophenyl)-L-cysteine (0.3 g, 1.24 mmol) was dissolved in a mixture of 10 mL of 98% formic acid and 2 mL of 30% hydrogen peroxide and stirred at room temperature for 48 h. After workup, the crude product was triturated with water, to give 0.21 g (62%) of fine white crystals, mp 133–136 °C dec, which were greater than 98% pure by ¹H NMR analysis. UV (0.01 M HCl): $\lambda_{max} = 276$ nm (sh) (log $\epsilon = 3.46$). IR (Nujol mull): ν 1154 and 1303 cm^{-1} (SO₂). ¹H NMR (D₂O, DCl): δ 4.22 (2 H, m, β-CH₂), 4.5 (1 H, dd, α-CH), 7.6–8.0 (4 H, m, aromatic). $[\alpha]^{23}_D$ +20.3 ($c = 1.00$, 1 M HCl).

H. Preparation of S-(4-Nitrophenyl)-L-cysteine S,S-Dioxide. S-(4-Nitrophenyl)-L-cysteine (0.65 g, 2.68 mmol) was reacted in 20 mL of 98% formic acid and 4 mL of 30% hydrogen peroxide for 12 h. Workup, followed by trituration with water, gave 0.58 g (79%) of a white solid, mp 153–156 °C (lit. 156–157 °C),[11] which was greater than 98% pure by ¹H NMR analysis. UV (0.01 M HCl): $\lambda_{max} = 252$ nm (log $\epsilon = 4.12$). IR (Nujol mull): ν 1150 and 1308 cm^{-1} (SO₂). ¹H NMR (D₂O, DCl): δ 3.90–4.09 (2 H, m, β-CH₂), 4.49–4.53 (1 H, dd, α-CH), 8.05–8.33 (4 H, m, aromatic). $[\alpha]^{23}_D$ +33.95 ($c = 1.025$, 1 M HCl).

I. Preparation of S-(2-Aminophenyl)-L-cysteine S,S-Dioxide. S-(2-Nitrophenyl)-L-cysteine S,S-dioxide (0.4 g, 1.46 mmol) was dissolved in 50 mL of formic acid, 45 mg of 10% Pd/C was added, and the mixture was hydrogenated at 40 psi for 30 min. The charcoal was removed by filtration through Celite, and the filtrate was concentrated in vacuo to give a light tan oil, which upon trituration with methanol gave 0.26 g (73%) of light-cream crystals, mp 156–158 °C dec, which were greater than 98% pure by ¹H NMR analysis. UV (0.01 M HCl): $\lambda_{max} = 243$ nm (log $\epsilon = 3.78$); 312 nm (log $\epsilon = 3.51$). IR (Nujol mull): ν 1144 and 1297 cm^{-1} (SO₂). ¹H NMR (D₂O, DCl): δ 4.35 (2 H, m, β-CH₂), 4.65 (1 H, dd, α-CH), 7.8–8.0 (4 H, m, aromatic). $[\alpha]^{23}_D$ +12.2 ($c = 1.00$, 1 M HCl). Anal. Calcd for C₉H₁₂N₂SO₄: C, 44.25; H, 4.95; N, 11.47. Found: C, 43.79; H, 4.88; N, 10.94.

(25) Hayaishi, O.; Stanier, R. Y. *J. Biol. Chem.* **1952**, *195*, 735.
(26) Moriguchi, M.; Yamamoto, T.; Soda, K. *Biochem. Biophys. Res. Commun.* **1971**, *44*, 752.
(27) Cleland, W. W. *Biochim. Biophys. Acta* **1964**, *67*, 173.
(28) Clark, M.; Cramer, R. D., III; Opdenbosch, N. V. *J. Comput. Chem.* **1989**, *10*, 982.

(29) Boyland, E.; Manson, D.; Nery, R. *J. Chem. Soc.* **1962**, 606–611.

J. Preparation of S-(4-Aminophenyl)-L-cysteine S,S-Dioxide. S-(4-Nitrophenyl)-L-cysteine S,S-dioxide (0.4 g, 1.46 mmol) was hydrogenated as described for S-(2-nitrophenyl)-L-cysteine S,S-dioxide. The brown crystalline product was recrystallized from hot ethanol to yield 0.31 g (87%) of light-tan crystals, which soften at 155 °C, mp 163–165 °C dec. UV (0.01 M HCl): λ_{max} = 270 nm (log ϵ = 4.19). IR (Nujol mull): ν 1139 and 1287 cm^{-1} (SO$_2$). ^{1}H NMR (D$_2$O, DCl): δ 3.98–4.17 (2 H, m, β-CH$_2$), 4.59–4.63 (1 H, dd, α-CH), 7.65–8.12 (4 H, dd,

aromatic). [α]^{23}_D +30.2 (c = 1.175, 1 M HCl).

Biosynthesis of Archaebacterial Ether Lipids. Formation of Ether Linkages by Prenyltransferases

Donglu Zhang and C. Dale Poulter*

Contribution from the Department of Chemistry, University of Utah, Salt Lake City, Utah 84112.
*Received August 17, 1992*

Abstract: Biosynthesis of (R)-2,3-di-O-phytanylglycerol (1), the core lipid of the membranes in the strict anaerobe *Methanobacterium thermoautotrophicum*, was studied in cell-free preparations. Two prenyltransferase activities were separated by ultracentrifugation. The cytosolic fraction contained activity for (S)-3-O-geranylgeranylglyceryl phosphate synthase (GGGP synthase), which catalyzes alkylation of (S)-glyceryl phosphate [(S)-3-OP] by geranylgeranyl diphosphate (5-OPP), while the pellet contained activity for (S)-2,3-O-digeranylgeranylglyceryl phosphate synthase (DGGGP synthase), which catalyzes alkylation of (S)-3-O-geranylgeranylglyceryl phosphate [(S)-12-OP] by 5-OPP. (S)-3-OP and 5-OPP were strongly preferred among the various compounds tested as prenyl acceptors [(S)-3-OP, (R)-3-OP, glycerol (3-OH), and dihydroxyacetone phosphate (4-OP)] and as prenyl donors [5-OPP, phytyl diphosphate (6-OPP), phytanyl diphosphate (7-OPP), farnesyl diphosphate (10-OPP), and farnesylgeranyl diphosphate (11-OPP)]. The products from the enzymatic reactions catalyzed by GGGP synthase and DGGGP synthase were characterized by hydrolysis of the phosphate moieties with alkaline phosphatase and comparisons of the glyceryl ethers with synthetic samples. These results demonstrate that the ether linkages in the core lipids of archaebacteria are formed in two distinct steps by a cytosolic GGGP synthase and a membrane-associated DGGGP synthase.
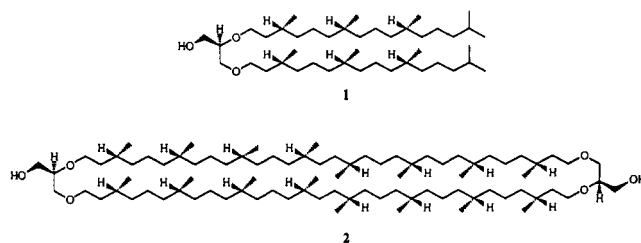
Introduction

According to a recent classification by Woese and co-workers,[1-3] all living organisms stem from the early divergence of a hypothetical progenitor into three primary kingdoms: archaebacteria, eubacteria, and eukaryotes. Designation of archaebacteria as a distinct kingdom was originally based on comparisons of ribosomal RNA sequences and is supported by several unique biochemical features, such as the construction of archaebacterial cell walls,[4] the structures of modified bases in archaebacterial tRNAs,[5] unique archaebacterial cofactors,[6] and unique structures for archaebacterial membrane lipids.[7] Archaebacteria are classified into three major phenotypes: extreme halophiles, methanogens, and thermoacidophiles,[3] which are typically confined to special ecological niches characterized by a high concentration of salt, high temperature, low pH, or absence of oxygen.

A distinctive molecular feature common to all archaebacteria is the nature of their core membrane lipids. In contrast to the membrane lipids composed of glyceryl esters of fatty acids found in eubacteria and eukaryotes, archaebacterial membranes contain isopranyl glyceryl ethers.[8,9] The two major hydrophobic com-

Scheme I. Synthesis of (S)-3-OP
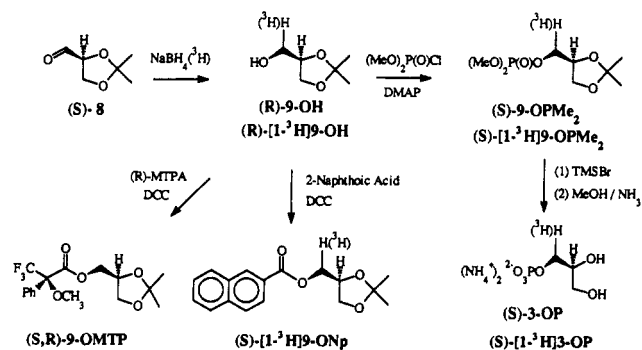
ponents typically found in archaebacterial lipids are a C$_{20}$ diether, (R)-2,3-di-O-(3R,7R,11R)-phytanylglycerol [(R)-1],[10] and a C$_{40}$ tetraether, (R)-2,3-di-O-(3R,7R,11R,15S,18S,22R,26R,30R)-biphytanyldiglycerol [(R)-2].[11] The absolute stereochemistry at C(2) of the glyceryl moieties is opposite to that of ester or ether lipids derived from fatty acids in eubacteria and eukaryotes.[12,13]

(1) Woese, C. R. *Sci. Am.* **1981,** *244,* 98–122.
(2) Fox, G. E.; Stackebrandt, E.; Hespell, R. B.; Gibson, J.; Maniloff, J.; Dyer, T. A.; Wolfe, R. S.; Balch, W. E.; Tanner, R. S.; Magrum, L. J.; Zablen, L. B.; Blakemore, R.; Gupta, R.; Bonen, L.; Lewis, B. J.; Stahl, D. A.; Luehrsen, K. R.; Chen, K. N.; Woese, C. R. *Science* (Washington, D.C.) **1980,** *209,* 457–463.
(3) Woese, C. R.; Magrum, L. J.; Fox, G. E. *J. Mol. Evol.* **1978,** *11,* 245–252.
(4) Kreisl, P.; Kandler, O. *Syst. Appl. Microbiol.* **1986,** *7,* 293–299.
(5) McClosky, J. A. *Syst. Appl. Microbiol.* **1986,** *7,* 246–252.
(6) Ankel-Fuchs, D.; Hüster, R.; Mörshel, E.; Albracht, S. P. J.; Thauer, R. K. *Syst. Appl. Microbiol.* **1986,** *7,* 383–387.
(7) De Rosa, M.; Gambacorta, A. *Prog. Lipid Res.* **1988,** *27,* 153–175.
(8) Langworthy, T. A.; Tornabene, T. G.; Holzer, G. *Zentralbl. Bakteriol. Mikrobiol. Hyg., Abt. 1, Orig. C* **1982,** *3,* 228–244.
(9) Langworthy, T. A.; Pond, J. L. *Syst. Appl. Microbiol.* **1986,** *7,* 253–257.

(10) Kates, M. *Prog. Chem. Fats Other Lipids* **1978,** *15,* 301–342.
(11) Heathcock, C. H.; Finkelstein, B. L.; Aoki, T.; Poulter, C. D. *Science* (*Washington, D.C.*) **1985,** *229,* 862–864.